Mathematics

http://www.aimspress.com/journal/Math

AIMS Mathematics, 10(5): 11234–11259.
DOI: 10.3934/math.2025509
Received: 26 February 2025
Revised: 30 April 2025
Accepted: 07 May 2025
Published: 16 May 2025

Research article

On weighted residual varextropy: characterization, estimation and application

Li Zhang[1] **and Bin Lu**[2,*]

[1] College of Mathematics and Statistics, Northwest Normal University, Lanzhou 730070, China
[2] Department of Mathematics, Lanzhou Jiaotong University, Lanzhou 730070, China

* **Correspondence:** Email: lubinnwnum@163.com.

Abstract: In recent years, the study of variability in uncertainty measures has gained significant interest in information theory. In this context, the concept of varextropy has been introduced and investigated by several researchers. This paper focuses on the study of weighted varextropy and introduces weighted residual varextropy, presenting a thorough examination of their theoretical properties. Specifically, we investigate the impact of monotonic transformations on these measures and derive various bounds. Additionally, we analyze the application of weighted varextropy within coherent systems and proportional hazard rates models. A non-parametric kernel-based method is introduced to estimate weighted (residual) varextropy, and the estimators' consistency and asymptotic normality are given. Finally, the effectiveness of this estimation method is demonstrated through simulations as well as analysis of a real-world data set, illustrating its potential applications in uncertainty analysis.

Keywords: variability measures; weighted residual varextropy; proportional hazard rates model; non-parametric estimation
Mathematics Subject Classification: 62G05, 94A17

1. Introduction

Quantifying the uncertainty tied to random variables is a fundamental task in various disciplines, including lifetime data analysis, experimental physics, and demography. To address this, a variety of information measures have been developed. Shannon [1] laid the foundation for information theory by introducing the concept of differential entropy for random variable X with probability density function (PDF) $f(x)$. The entropy $H(X)$ is given by

$$H(X) = -E\big(\log(f(X))\big) = -\int_0^{\infty} f(x)\log f(x)\mathrm{d}x. \tag{1.1}$$

Here, the natural logarithm is used with the convention $0 \log 0 = 0$. As noted by [2], entropy alone does not comprehensively capture the information within a distribution. As an alternative, they introduced extropy, a complementary measure of uncertainty, which is

$$J(X) = E\Big(-\frac{1}{2}f(X)\Big) = -\frac{1}{2}\int_0^\infty f^2(x)\mathrm{d}x.$$

Extropy, $J(X)$, is particularly useful for quantifying uncertainty related to the lifetime of systems. However, for certain scenarios, such as when the current age of a system is known, extropy alone may be insufficient to assess the remaining uncertainty. Specifically, for a unit that has survived up to a given time t, it becomes essential to consider residual extropy as an appropriate measure. Qiu and Jia [3] formalized the residual extropy, which is defined as

$$J(X;t) = -\frac{1}{2}\int_t^\infty \left(\frac{f(x)}{\bar{F}(t)}\right)^2 \mathrm{d}x, \tag{1.2}$$

where $f_{X_t}(x) = f(x)/\bar{F}(t)$ denotes the PDF of $X_t = [X - t|X > t]$, and $\bar{F}(t)$ is the survival function of X. The measures $J(X)$ and $J(X;t)$ defined here give equal importance to each event and depend solely on the probability, regardless of the values of random variables, ensuring the measure that remains shift-independent. Nevertheless, in practical applications, such as reliability analysis or mathematical neurobiology, addressing shift-dependent information measures becomes essential. To tackle this challenge, researchers have introduced weighted information measures, which can account for specific contexts. Sathar and Nair [4] developed weighted variants of extropy measures to address these concerns. Specifically, they defined the weighted extropy (WEx) and the weighted residual extropy (WREX) as

$$J^w(X) = -\frac{1}{2}\int_0^\infty w(x)f^2(x)\mathrm{d}x \tag{1.3}$$

and

$$J^w(X;t) = -\frac{1}{2}\int_t^\infty w(x)\left(\frac{f(x)}{\bar{F}(t)}\right)^2 \mathrm{d}x, \tag{1.4}$$

respectively, where the weighting function $w(x)$ represents the variability of the weighted information content associated with X. It is worth mentioning that as t approaches zero, $J^w(X;t)$ converges to $J^w(X)$. Various authors have explored measures of extropy measures and their practical uses. Qiu [5] analyzed characterization properties, monotonic behavior, and lower bounds of extropy for order statistics and record values. Krishnan et al. [6] and Nair and Sathar [7] investigated interrelations among extropy and derived results linking them to L-moments. For additional research on extropy and its application, please refer to [8–10].

The concept of varextropy has been introduced as a complementary measure to Shannon entropy for quantifying uncertainty. The varextropy of X is (see [11])

$$VJ(X) = Var\Big(-\frac{1}{2}f(X)\Big) = \frac{1}{4}E\left(f^2(X)\right) - J^2(X) = \frac{1}{4}\left(\int_0^\infty f^3(x)\mathrm{d}x - \left(\int_0^\infty f^2(x)\mathrm{d}x\right)^2\right).$$

As noted by the authors, when two variables share the same extropy, varextropy provides a valuable tool for determining which extropy is more appropriate for measuring uncertainty. Moreover, it has been argued that varextropy is often more adaptable than varentropy, as it does not rely on distributional parameters in specific models. Vaselabadi et al. [11] extended these concepts to study the residual varextropy of X at time t, given by

$$VJ(X;t) = \frac{1}{4}E\left(f_t^2(X_t)\right) - (J(X;t))^2. \tag{1.5}$$

Recently, Chaudhary and Gupta [12] introduced the notion of weighted varextropy (WVEx), given by

$$\begin{aligned} VJ^w(X) &= Var\left(-\frac{1}{2}w(X)f(X)\right) \\ &= \frac{1}{4}\left(E\left(w^2(X)f^2(X)\right) - E^2\left(w(X)f(X)\right)\right) \\ &= \frac{1}{4}\left(\int_0^\infty w^2(x)f^3(x)\mathrm{d}x - \left(\int_0^\infty w(x)f^2(x)\mathrm{d}x\right)^2\right). \end{aligned} \tag{1.6}$$

Saha and Kayal [13] introduced weighted varentropy (WVE) and weighted residual varentropy (WRVE) for random variables and examined their theoretical properties. Vaselabadi et al. [11] highlighted an important distinction: WVE lacks affine invariance, whereas varentropy retains this property. This limitation arises because varentropy and varextropy are sometimes unable to capture the variability in the information content of a random process across different time points. To address this shortcoming, measures such as WVE and WVEx have been proposed.

The most existing research has primarily focused on the properties of WVEx and residual varextropy. In this paper, we further explore some properties of WVEx. As noted by Asadi et al. [14], if X represents the lifetime of a new unit, the classical entropy $H(X)$ may not adequately capture the uncertainty regarding the unit's residual lifetime. In such cases, it becomes essential to consider residual varextropy. In practical applications such as lifetime analysis, classical entropy or extropy provides a global perspective on uncertainty, treating all values of the random variable equally. However, in many real-world contexts, particularly in reliability and survival analysis, the uncertainty associated with the residual life beyond a certain threshold is of greater relevance. In engineering systems, once a system has operated up to time t, understanding the variability and uncertainty of its remaining lifetime becomes crucial for maintenance planning and risk assessment. Weighted residual varextropy (WRVEx) offers a localized measure specifically tailored to the residual distribution, providing more actionable insights. In medical applications, patients who have survived beyond a critical period often present different risk profiles. Weighted measures such as WVEx and WRVEx enable emphasis on particular survival times (e.g., long-term survivors), delivering more clinically meaningful evaluations compared to uniform entropy-based measures.

The paper is structured as follows: Section 2 explores several properties of WVEx, including closed-form expressions for WVEx in specific distributions. We also derive the WVEx under affine transformations and explore its various bounds. Section 3 proposes WRVEx and presents several findings, including bounds for WRVEx. Additionally, we investigate WRVEx under general monotonic transformations and the proportional hazard rates (PHR) model. In Section 4, we examine the WVEx of coherent systems and present several proposed bounds. Section 5 provides insights into non-parametric estimation of both WVEx and WRVEx using real and simulated datasets. Section 6 presents an analysis of a real dataset to illustrate the proposed methods. Finally, Section 7 summarizes this paper.

Throughout this work, it is assumed that all random variables are absolutely continuous and non-negative. Furthermore, the terms "increasing" and "decreasing" are used to refer to functions that are non-decreasing and non-increasing, respectively.

2. Weighted varextropy

It is often challenging to obtain an explicit closed-form expression for the WVEx. In such situations, transformations can be utilized to determine the WVEx of a transformed random variable by leveraging the WVEx of a known distribution. Theorem 2.1 provides a practical solution in this regard.

Theorem 2.1. *Let X be a random variable with PDF $f(x)$, and consider the affine-transformed variable $Y = aX + b$, where $a > 0$ and $b \geq 0$. The WVEx of Y is given by*

$$VJ^y(Y) = VJ^x(X) + \left(\frac{b}{a}\right)^2 VJ(X) + \frac{b}{2a}\left(E\left(Xf^2(X)\right) - 4J^x(X)J(X)\right),$$

where $VJ^x(X)$ denotes the WVEx of X with $w(x) = x$.

Proof. Let $Y = aX + b$, where $a > 0$. Then the PDF of Y is given by the standard transformation formula

$$g(y) = \frac{1}{a} f\left(\frac{y-b}{a}\right), \quad y > b.$$

By (1.6), it follows that

$$VJ^y(Y) = \frac{1}{4}\int_0^\infty y^2 g^3(y)\mathrm{d}y - (J^y(Y))^2, \tag{2.1}$$

where

$$J^y(Y) = -\frac{1}{2}\int_0^\infty y g^2(y)\,\mathrm{d}y = -\frac{1}{2}\int_b^\infty y\left(\frac{1}{a}f\left(\frac{y-b}{a}\right)\right)^2 \mathrm{d}y = -\frac{1}{2a^2}\int_b^\infty y f^2\left(\frac{y-b}{a}\right)\mathrm{d}y. \tag{2.2}$$

Now, perform the change of variable $x = \frac{y-b}{a}$, which implies $y = ax + b$, and $\mathrm{d}y = a\mathrm{d}x$. Substituting into (2.2), we have

$$\begin{aligned} J^y(Y) &= -\frac{1}{2a^2}\int_0^\infty (ax+b) f^2(x)\cdot a\mathrm{d}x \\ &= -\frac{1}{2a}\int_0^\infty (ax+b) f^2(x)\mathrm{d}x \\ &= -\frac{1}{2}\int_0^\infty x f^2(x)\mathrm{d}x - \frac{b}{2a}\int_0^\infty f^2(x)\mathrm{d}x \\ &= J^x(X) + \frac{b}{a}J(X). \end{aligned} \tag{2.3}$$

Note that

$$\int_0^\infty y^2 g^3(y)\mathrm{d}y = \int_0^\infty \left(\frac{ax+b}{a}\right)^2 f^3(x)\mathrm{d}x \tag{2.4}$$

$$= \int_0^\infty x^2 f^3(x)\mathrm{d}x + \frac{2b}{a}\int_0^\infty x f^3(x)\mathrm{d}x + \left(\frac{b}{a}\right)^2 \int_0^\infty f^3(x)\mathrm{d}x. \tag{2.5}$$

Substituting Eqs (2.3) and (2.4) into (2.1) yields the required result, completing the proof.

Remark 2.1. *According to [4], X and $X+b$ possess different weighted extropy despite having identical extropy. For $Y = aX + b$, $J(Y) = \frac{1}{a}J(X)$ and $J^w(Y) = J^w(X) + \frac{b}{a}J(X)$; thus, when $a = 1$, $J(Y) = J(X)$ while $J^w(Y) \neq J^w(X)$. They also show that X and aX have identical weighted extropy, but their extropies differ. As discussed in [11], $VJ(Y) = \frac{1}{a^2}VJ(X)$, Theorem 2.1 also highlights cases where, for $b = 0$, X and $X + b$ have distinct WVEx even though their varextropy remains identical.*

In the following, we compute WVEx defined in (1.6) with $w(x) = x$ for some continuous distributions, which are derived under the assumption that the underlying random variables are absolutely continuous and possess finite moments required for the existence of the weighted expectations. Table 1 presents the WVEx values for several widely used distributions.

Table 1. WVEx for various distributions.

Distribution	$f(z)$	$VJ^w(X)$
Uniform (a, b)	$\frac{1}{(b-a)}, \quad a < z < b$	$\frac{1}{48}$
Exponential (θ)	$\theta e^{-\theta z}, \quad 0 < z < \infty$	$\frac{5}{1728}$
Gamma (α,β)	$\frac{e^{-\beta z} z^{\alpha-1}\beta^\alpha}{\Gamma(\alpha)}, \quad 0 < z < \infty$	$\frac{1}{4}\left[\frac{\Gamma(3\alpha)}{3^{3\alpha}\Gamma(\alpha)^3} - \frac{\Gamma(2\alpha)^2}{2^{4\alpha}\Gamma(\alpha)^4}\right]$
Beta (α, θ)	$\frac{z^{\alpha-1}(1-z)^{\theta-1}}{B(\alpha,\theta)}, \quad 0 < z < 1$	$\frac{1}{4}\left[\frac{B(3\alpha,3\theta-2)}{B(\alpha,\theta)^3} - \frac{B(2\alpha,2\theta-1)^2}{B(\alpha,\theta)^4}\right]$
Power (α, λ)	$\alpha\lambda^\alpha z^{\alpha-1}, \quad 0 < z \leq \frac{1}{\lambda}$	$\frac{1}{48}\alpha^2$
Rayleigh (σ)	$\frac{z}{\sigma^2}e^{-\frac{z^2}{2\sigma^2}}, \quad 0 < z < \infty$	$\frac{5}{432}$

Here, we provide detailed derivations of WVEx for the Gamma, Beta and Power distributions.
(i) Let X follow Gamma (α,β), then, we have

$$\begin{aligned} VJ^w(X) &= \frac{1}{4}\left(\int_0^\infty w^2(x)f^3(x)\mathrm{d}x - \left(\int_0^\infty w(x)f^2(x)\mathrm{d}x\right)^2\right) \\ &= \frac{1}{4}\left(\int_0^\infty x^2\Big(\frac{e^{-\beta z}x^{\alpha-1}\beta^\alpha}{\Gamma(\alpha)}\Big)^3\mathrm{d}x - \left(\int_0^\infty x\Big(\frac{e^{-\beta x}x^{\alpha-1}\beta^\alpha}{\Gamma(\alpha)}\Big)^2\mathrm{d}x\right)^2\right) \\ &= \frac{3^{-3\alpha}\Gamma(\alpha)\Gamma(3\alpha) - 4^{-2\alpha}\Gamma(2\alpha)^2}{4\Gamma(\alpha)^4} \end{aligned}$$

$$
\begin{aligned}
&= \frac{1}{4}\left(\frac{3^{-3\alpha}\Gamma(\alpha)\Gamma(3\alpha)}{\Gamma(\alpha)^4} - \frac{4^{-2\alpha}\Gamma(2\alpha)^2}{\Gamma(\alpha)^4}\right)\\
&= \frac{1}{4}\left(\frac{\Gamma(3\alpha)}{3^{3\alpha}\Gamma(\alpha)^3} - \frac{\Gamma(2\alpha)^2}{2^{4\alpha}\Gamma(\alpha)^4}\right).
\end{aligned}
$$

(ii) Let X follow Beta (α, θ); then, we have

$$
\begin{aligned}
VJ^w(X) &= \frac{1}{4}\left(\int_0^1 w^2(x)f^3(x)\mathrm{d}x - \left(\int_0^1 w(x)f^2(x)\mathrm{d}x\right)^2\right)\\
&= \frac{1}{4}\left(\int_0^1 x^2\left(\frac{x^{\alpha-1}(1-x)^{\theta-1}}{B(\alpha,\theta)}\right)^3\mathrm{d}x - \left(\int_0^1 x\left(\frac{x^{\alpha-1}(1-x)^{\theta-1}}{B(\alpha,\theta)}\right)^2\mathrm{d}x\right)^2\right)\\
&= \frac{\dfrac{B(\alpha,\theta)\Gamma(3\alpha)\Gamma(3\theta-2)}{\Gamma(3\alpha+3\theta-2)} - \dfrac{\Gamma(2\alpha)^2\Gamma(2\theta-1)^2}{\Gamma(2\alpha+2\theta-1)^2}}{4B(\alpha,\theta)^4}\\
&= \frac{B(\alpha,\theta)B(3\alpha,3\theta-2) - B(2\alpha,2\theta-1)^2}{4B(\alpha,\theta)^4}.
\end{aligned}
$$

Note that

$$
B(\alpha,\theta) = \frac{\Gamma(\alpha)\Gamma(\theta)}{\Gamma(\alpha+\theta)},
$$

then we have

$$
\frac{\Gamma(2\alpha)^2\Gamma(2\theta-1)^2}{\Gamma(2\alpha+2\theta-1)^2} = B(2\alpha, 2\theta-1)^2,
$$

and

$$
\frac{\Gamma(3\alpha)\Gamma(3\theta-2)}{\Gamma(3\alpha+3\theta-2)} = B(3\alpha, 3\theta-2).
$$

Thus,

$$
\begin{aligned}
\frac{\dfrac{B(\alpha,\theta)\Gamma(3\alpha)\Gamma(3\theta-2)}{\Gamma(3\alpha+3\theta-2)} - \dfrac{\Gamma(2\alpha)^2\Gamma(2\theta-1)^2}{\Gamma(2\alpha+2\theta-1)^2}}{4B(\alpha,\theta)^4} &= \frac{B(\alpha,\theta)B(3\alpha,3\theta-2) - B(2\alpha,2\theta-1)^2}{4B(\alpha,\theta)^4}\\
&= \frac{1}{4}\left(\frac{B(\alpha,\theta)B(3\alpha,3\theta-2)}{B(\alpha,\theta)^4} - \frac{B(2\alpha,2\theta-1)^2}{B(\alpha,\theta)^4}\right)\\
&= \frac{1}{4}\left(\frac{B(3\alpha,3\theta-2)}{B(\alpha,\theta)^3} - \frac{B(2\alpha,2\theta-1)^2}{B(\alpha,\theta)^4}\right).
\end{aligned}
$$

(iii) Let X follow Power (α, λ), then we have

$$
\begin{aligned}
VJ^w(X) &= \frac{1}{4}\left(\int_0^{\frac{1}{\lambda}} w^2(x)f^3(x)\mathrm{d}x - \left(\int_0^{\frac{1}{\lambda}} w(x)f^2(x)\mathrm{d}x\right)^2\right)\\
&= \frac{1}{4}\left(\int_0^{\frac{1}{\lambda}} x^2\left(\alpha\lambda^\alpha z^{\alpha-1}\right)^3\mathrm{d}x - \left(\int_0^{\frac{1}{\lambda}} x\left(\alpha\lambda^\alpha z^{\alpha-1}\right)^2\mathrm{d}x\right)^2\right)\\
&= \frac{\alpha^2}{48}.
\end{aligned}
$$

Example 2.1. Let X follow Gamma and Beta distribution, respectively. Figures 1 and 2 depict the variation of $VJ^w(X)$ concerning distribution parameters.

Figure 1 indicates that $VJ^w(X)$ varies with α; as α increases, $VJ^w(X)$ also increases steadily.

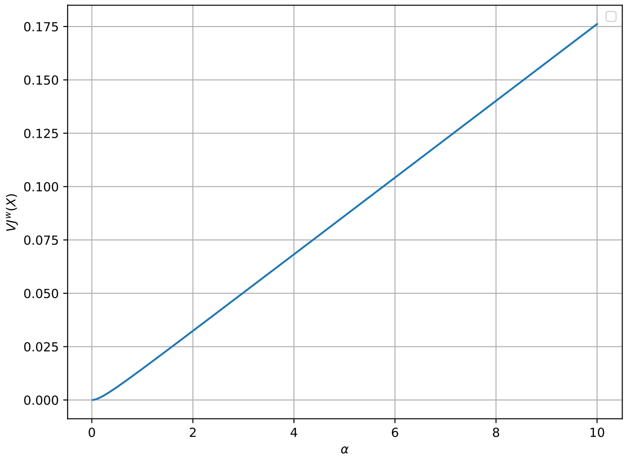

Figure 1. Plots of $VJ^w(X)$ for Gamma distribution.

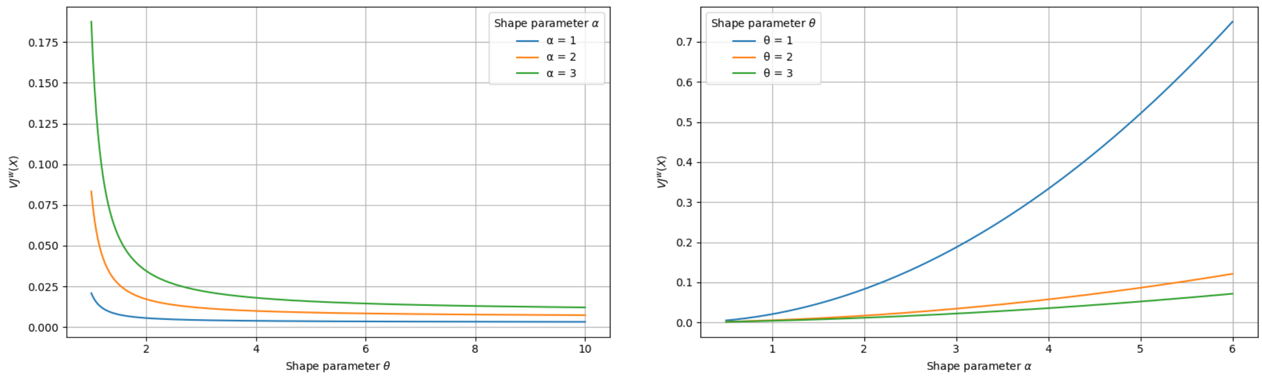

(a) $VJ^w(X)$ with respect to θ for $\alpha = 1, 2, 3$.

(b) $VJ^w(X)$ with respect to α for $\theta = 1, 2, 3$.

Figure 2. Plots of $VJ^w(X)$ for Beta distribution with different shape parameters α and θ.

From Figure 2, it is evident that $VJ^w(X)$ depends on both α and θ. As θ increases, $VJ^w(X)$ decreases more sharply, with higher α values causing steeper declines. Conversely, increasing α leads to an increase in $VJ^w(X)$, and $VJ^w(X)$ shows stronger sensitivity to α for larger θ. The effect of α is more pronounced for larger θ, while smaller θ results in a more gradual change of $VJ^w(X)$ as α varies.

Sometimes, obtaining the closed-form expression of WVEx is not feasible. In such instances, bounds can provide valuable insight into the variability measure. The next theorem establishes bounds for the WVEx with $w(x) = x$. The proof is straightforward and hence omitted.

Theorem 2.2. *Let X be a random variable with PDF $f(x)$, such that*

$$\frac{1}{x^3+3} \le f(x) \le 1,$$

then

$$\frac{1}{4}\left((E\left(w^2(X)f^2(X)\right) - (E(X))^2\right) \le VJ^w(X) \le -\frac{1}{2}J^{w_1}(X) - \frac{1}{4}\left(E\Big(\frac{X}{X^3+3}\Big)\right)^2,$$

where $J^{w_1}(X)$ is the WEx with $w_1(x) = x^2$.

Proof. According to Eq (1.6), for $w(x) = x$, we have

$$VJ^w(X) = \frac{1}{4}\left(\int_0^\infty x^2 f^3(x)\mathrm{d}x - \left(\int_0^\infty xf^2(x)\mathrm{d}x\right)^2\right).$$

For the first integral, we obtain that

$$\int_0^\infty x^2 f^3(x)\mathrm{d}x \le \int_0^\infty x^2 f(x)\mathrm{d}x = E(X^2) = J^{w_1}(X),$$

where $w_1(x) = x^2$, and thus

$$\int_0^\infty x^2 f^3(x)\mathrm{d}x \le J^{w_1}(X).$$

Moreover, since $f(x) \ge \frac{1}{x^3+3}$, we obtain

$$\int_0^\infty xf^2(x)\mathrm{d}x \ge \int_0^\infty x\left(\frac{1}{x^3+3}\right)^2 \mathrm{d}x = E\left(\frac{X}{(X^3+3)^2}\right),$$

then

$$\left(\int_0^\infty xf^2(x)\mathrm{d}x\right)^2 \ge \left(E\left(\frac{X}{(X^3+3)^2}\right)\right)^2.$$

We then obtain the upper bound

$$VJ^w(X) \le -\frac{1}{2}J^{w_1}(X) - \frac{1}{4}\left(E\left(\frac{X}{X^3+3}\right)\right)^2.$$

On the other hand, using the upper bound $f(x) \le 1$, we obtain

$$\int_0^\infty x^2 f^3(x)\mathrm{d}x \ge \int_0^\infty x^2\left(\frac{1}{x^3+3}\right)^3 \mathrm{d}x,$$

and

$$\int_0^\infty xf^2(x)\mathrm{d}x \le \int_0^\infty x\cdot 1^2\mathrm{d}x = E(X).$$

Thus,

$$VJ^w(X) \ge \frac{1}{4}\left(E\left(x^2 f^3(x)\right) - (E(X))^2\right).$$

Combining the two bounds yields the desired result. □

The condition $\frac{1}{x^3+3} \leq f(x) \leq 1$ assumed in Theorem 2.2 ensures that the probability density function $f(x)$ is bounded above and below in a controlled manner. In particular, the upper bound restricts the distribution from having excessively sharp peaks, while the lower bound guarantees that the density does not decay too quickly at infinity. This condition is satisfied by a variety of distributions with moderately heavy tails; the following remark is presented to illustrate the condition in Theorem 2.2.

Remark 2.2. *(i) Let X follow a Lomax distribution with CDF* $F(x) = 1 - \left(1 + \frac{x}{a}\right)^{-b}$, $a > 0,\ b > 0$. *Figure 3(a) illustrates that the condition*

$$\frac{1}{x^3 + 3} \leq f(x) \leq 1$$

holds for $a = 2$ *and* $b = 1.5$.

(ii) Let X follow a Pareto distribution with PDF

$$f(x) = ba^b x^{-b-1}.$$

Figure 3(b) illustrates that the condition in Theorem 2.2 also holds for $a = 0.4$ *and* $b = 0.5$.

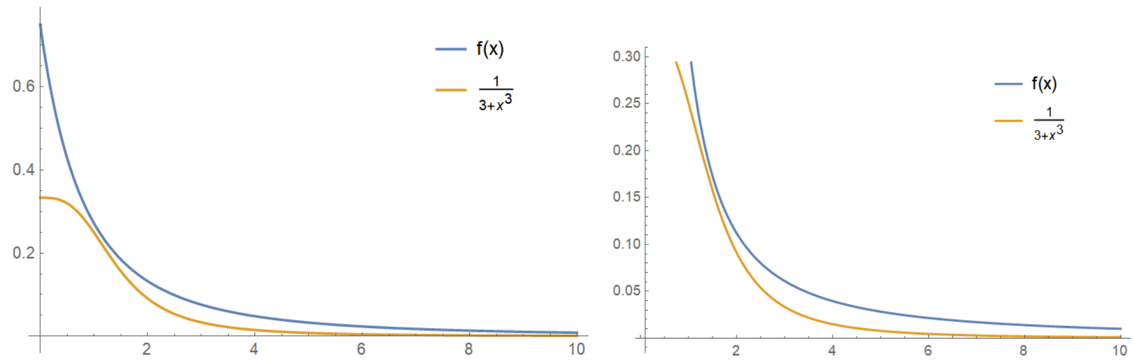

(a) Lomax PDF and $1/(x^3 + 3)$. (b) Pareto PDF and $1/(x^3 + 3)$.

Figure 3. Illustrate the condition $1/(x^3 + 3) \leq f(x) \leq 1$.

In the following, we examine the WVEx under monotonic transformations and explore its fundamental properties.

Theorem 2.3. *Let* $Y = \varphi(X)$, *where* $\varphi(x)$ *be a strictly monotone, continuous, and differentiable function. Then, the WVEx of Y is*

$$VJ^y(Y) = \begin{cases} VJ^{\frac{\varphi}{\varphi'}}(X), & \text{if } \varphi \text{ is strictly increasing;} \\ -\frac{1}{4}E\left(\frac{\varphi^2(X)}{\varphi'(X)^2}f^2(X)\right) - J^{\frac{\varphi}{\varphi'}}(X), & \text{if } \varphi \text{ is strictly decreasing,} \end{cases}$$

where $J^{\frac{\varphi}{\varphi'}}(X)$ *and* $VJ^{\frac{\varphi}{\varphi'}}(X)$ *with* $w(x) = \varphi(x)/\varphi'(x)$ *are defined as* (1.3) *and* (1.6), *respectively.*

Proof. Consider the first case where $\varphi(x)$ is strictly increasing. By (1.6), the WVEx of $Y = \varphi(X)$ is given by

$$VJ^y(Y) = \frac{1}{4}\left(\int_0^\infty y^2 \frac{f^3(\varphi^{-1}(y))}{(\varphi'(\varphi^{-1}(y)))^3}dy - \left(\int_0^\infty y\frac{f^2(\varphi^{-1}(y))}{(\varphi'(\varphi^{-1}(y)))^2}dy\right)^2\right). \tag{2.6}$$

Substituting $y = \varphi(x)$ into the above expression simplifies the right-hand side, yielding the desired result.

When φ is strictly decreasing, the transformation $Y = \varphi(X)$ implies that

$$F_Y(y) = P(Y \leq y) = P(\varphi(X) \leq y) = P(X \geq \varphi^{-1}(y)) = 1 - F_X(\varphi^{-1}(y)).$$

Thus, the PDF of Y is

$$f_Y(y) = \left|\frac{\mathrm{d}}{\mathrm{d}y}F_Y(y)\right| = \left|-f_X(\varphi^{-1}(y)) \cdot \frac{\mathrm{d}}{\mathrm{d}y}\varphi^{-1}(y)\right| = f_X(\varphi^{-1}(y))\left|\frac{\mathrm{d}}{\mathrm{d}y}\varphi^{-1}(y)\right|.$$

Since φ is strictly decreasing, we have $\varphi'(x) < 0$ for all x, and thus

$$\frac{\mathrm{d}}{\mathrm{d}y}\varphi^{-1}(y) = \frac{1}{\varphi'(\varphi^{-1}(y))} < 0.$$

Therefore,

$$f_Y(y) = \frac{f_X(\varphi^{-1}(y))}{|\varphi'(\varphi^{-1}(y))|}.$$

Note that $y = \varphi(x)$; we have

$$f_Y(\varphi(x)) = \frac{f_X(x)}{|\varphi'(x)|}.$$

Thus,

$$\int_0^{\infty} y^2 f_Y^3(y)\mathrm{d}y = \int_0^{\infty} \varphi^2(x)\left(\frac{f_X(x)}{|\varphi'(x)|}\right)^3 |\varphi'(x)|\mathrm{d}x = \int_0^{\infty} \frac{\varphi^2(x)}{|\varphi'(x)|^2} f_X^3(x)\mathrm{d}x,$$

and

$$\left(\int_0^{\infty} y f_Y^2(y)\mathrm{d}y\right)^2 = \left(\int_0^{\infty} \varphi(x)\left(\frac{f_X(x)}{|\varphi'(x)|}\right)^2 |\varphi'(x)|\mathrm{d}x\right)^2 = \left(\int_0^{\infty} \frac{\varphi(x)}{|\varphi'(x)|} f_X^2(x)\mathrm{d}x\right)^2.$$

Therefore,

$$VJ^y(Y) = \frac{1}{4}\left(\int_0^{\infty} \frac{\varphi^2(x)}{(\varphi'(x))^2} f_X^3(x)\mathrm{d}x - \left(\int_0^{\infty} \frac{\varphi(x)}{\varphi'(x)} f_X^2(x)\mathrm{d}x\right)^2\right).$$

By simplifying, we finally obtain

$$VJ^y(Y) = -\frac{1}{4}E\left(\frac{\varphi^2(X)}{(\varphi'(X))^2} f^2(X)\right) - J^{\frac{\varphi}{\varphi'}}(X).$$

The next remark demonstrates how WVEx behaves under scale and location transformations.

Remark 2.3. *(a) If $Y = aX$, $a > 0$, then*

$$VE^{ax}(aX) = VJ^{\frac{\varphi}{\varphi'}}(X) = VJ^x(X).$$

(b) If $Y = X + b$,, then

$$VJ^{\varphi}(X + b) = VJ^{\frac{\varphi}{\varphi'}}(X) = VJ^x(X) + b^2 VJ(X) + \frac{b}{2}\left(E\left(Xf^2(X)\right) - 4J^x(X)J(X)\right),\ b \geq 0.$$

3. Weighted residual varextropy

Inspired by [12], this section introduces the WRVEx as a natural generalization of the residual varextropy (RVEx), aiming to provide a more flexible tool for measuring uncertainty in the residual lifetime of random variable X. By introducing a weight function $w(x)$, we allow differential emphasis across the support of X, thereby enabling a more nuanced quantification of residual uncertainty. For a weight function $w(x)$, the WRVEx of X can be expressed as

$$VJ^w(X;t) = \frac{1}{4}\Big(\int_t^{\infty} w^2(x) \left(\frac{f(x)}{\bar{F}(t)}\right)^3 \mathrm{d}x - \Big(\int_t^{\infty} w(x) \left(\frac{f(x)}{\bar{F}(t)}\right)^2 \mathrm{d}x\Big)^2\Big). \tag{3.1}$$

Moreover, as $t \to 0$, the WRVEx converges to the weighted varextropy, i.e., $VJ^w(X;t) \to VJ^w(X)$, reflecting the global weighted uncertainty of X. The weighted varextropy measures the overall uncertainty of X under a weight function $w(x)$, while WRVEx focuses on the residual distribution beyond a specified threshold t.

Next, we present the WRVEx given by (3.1) with $w(x) = x$ for various commonly used distributions.

Example 3.1. (i) Suppose X is uniformly distributed over the interval (a, b). In this case, we have $VJ^w(X;t) = 1/48$, which matches the WVEx of $U(a, b)$.
(ii) Suppose X follows an exponential distribution with parameter λ. Then, the WRVEx is

$$VJ^w(X;t) = \frac{12\lambda t(3\lambda t - 1) + 5}{1728}.$$

(iii) Let X follow a Rayleigh distribution with PDF

$$f(x) = \frac{x}{\sigma^2} e^{-\frac{x^2}{2\sigma^2}},\ 0 < x < \infty.$$

Then, we have

$$VJ^w(X;t) = \frac{5\sigma^4 + 9t^4 - 6\sigma^2 t^2}{432\sigma^4}.$$

Figure 4 illustrates how the variation of $VJ^w(X;t)$ depends on t and parameters of exponential and Rayleigh distributions. The plots demonstrate that $VJ^w(X;t)$ increases sharply as t increases. Larger values of λ and σ result in a slower increase of $VJ^w(X;t)$ as t grows.

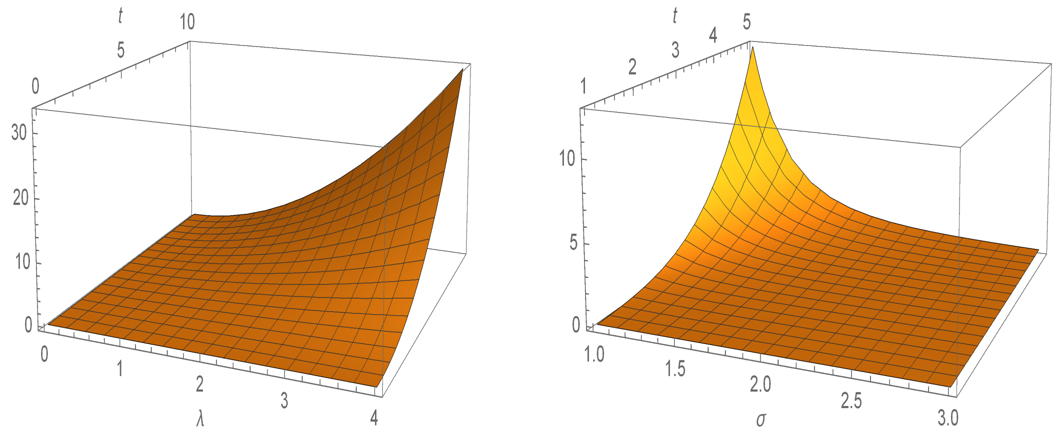

(a) Exponential distribution

(b) Rayleigh distribution

Figure 4. Plots of $VJ^w(X;t)$ for two distributions.

The result below presents a clear expression for the derivative of WRVEx with respect to t.

Theorem 3.1. *For any $t > 0$, it holds that*

$$\frac{d}{dt}VJ^w(X;t) = \frac{1}{4}\left(w^2(t)r^3(t) + w(t)r^2(t)\right) + \frac{3}{4}\frac{r(t)}{\bar{F}^2(t)}E\left(w^2(X)f(X)|X > t\right) - \frac{1}{2}\frac{r(t)}{\bar{F}(t)}E(w(X)|X > t).$$

Proof. Based on (3.1), we can obtain that

$$\begin{aligned}
\frac{d}{dt}VJ^w(X;t) &= \frac{d}{dt}\left(\frac{1}{4}\int_t^\infty w^2(x)\left(\frac{f(x)}{\bar{F}(t)}\right)^3 \mathrm{d}x - (J^w(X;t))^2\right) \\
&= \frac{1}{4}w^2(t)\left(\frac{f(t)}{\bar{F}(t)}\right)^3 + \frac{3}{4}\frac{f(t)}{\bar{F}(t)}\int_t^\infty w^2(x)\left(\frac{f(x)}{\bar{F}(t)}\right)^2 \mathrm{d}x + w(t)\left(\frac{f(t)}{\bar{F}(t)}\right)^2 \\
&\quad -2\frac{f(t)}{\bar{F}(t)}\int_t^\infty w(x)\left(\frac{f(x)}{\bar{F}(t)}\right)^2 \mathrm{d}x - \frac{1}{2}\int_t^\infty w(x)\left(\frac{f(x)}{\bar{F}(t)}\right)^2 \mathrm{d}x \\
&= \frac{1}{4}w^2(t)r^3(t) + \frac{3}{4}\frac{r(t)}{\bar{F}^2(t)}\int_t^\infty w^2(x)f^2(x)\mathrm{d}x + \frac{1}{4}w(t)r^2(t) \\
&\quad -\frac{1}{2}\frac{r(t)}{\bar{F}(t)}\int_t^\infty w(x)f(x)\mathrm{d}x - \frac{1}{2}\int_t^\infty w(x)\left(\frac{f(x)}{\bar{F}(t)}\right)^2 \mathrm{d}x \\
&= \frac{1}{4}w^2(t)r^3(t) + \frac{3}{4}\frac{r(t)}{\bar{F}^2(t)}E\left(w^2(X)f(X)|X > t\right) + \frac{1}{4}w(t)r^2(t) \\
&\quad -\frac{1}{2}\frac{r(t)}{\bar{F}(t)}E(w(X)|X > t) - \frac{1}{2}\frac{1}{\bar{F}^2(t)}E\left(w(X)f^2(X)|X > t\right).
\end{aligned}$$

The following theorem establishes bounds for the WRVEx.

Theorem 3.2. *If the PDF $f(x)$ of X satisfies*

$$\frac{1}{x^3+3} \leq f(x) \leq 1,$$

then

$$-\frac{1}{2\bar{F}(t)}J^{w_2}(X;t)-(J^x(X;t))^2\leq VJ^x(X;t)\leq -\frac{1}{2\bar{F}(t)}J^{w_1}(X;t)-\frac{1}{4\bar{F}^4(t)}\left(E\left(\frac{X}{X^3+3}\middle|X>t\right)\right)^2,$$

where $J^{w_1}(X;t)$ *and* $J^{w_2}(X;t)$ *are defined with* $w_1(x)=x^2$ *and* $w_2(x)=x^2/(x^3+3)$ *as in* (1.4).

Example 3.2. Suppose X follows the Lomax distribution with CDF

$$F(x)=1-\left(1+\frac{x}{a}\right)^{-b}.$$

For $a=4$ and $b=2$, the condition specified in Theorem 3.2 is satisfied. Figure 5 displays $VJ^x(X;t)$ and its two bounds, illustrating the result in Theorem 3.2.

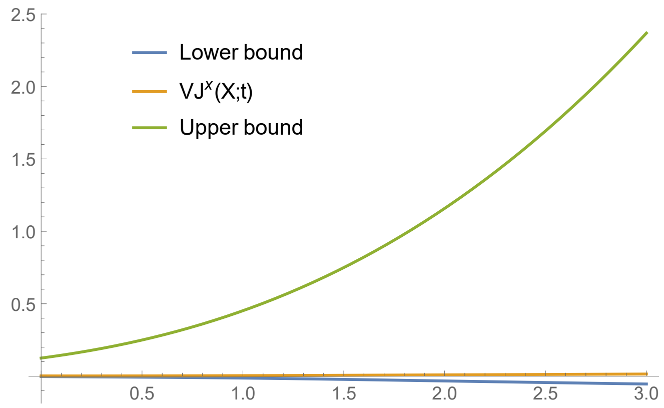

Figure 5. Graph of WRVEx and its bounds.

Theorem 3.3. For a random variable X, the following holds:

$$\frac{t}{4\bar{F}^3(t)}E(Xf^2(X)|X>t)-(J^x(X;t))^2\leq VJ^x(X;t)\leq\frac{1}{4\bar{F}^3(t)}E\left(X^2f^2(X)|X>t\right)-tJ(X;t)J^x(X;t),$$

where $J(X;t)$ is defined in (1.2), and $J^x(X;t)$ is defined in (1.4) with $w(x)=x$.

Proof. According to Lemma 2 of [13], $J^x(X;t)\leq tJ(X;t)$. The remainder of the proof follows from simple transformations and is omitted for brevity.

We now present a lower bound for the WRVEx, expressed using the variance of the residual life (VRL), denoted as $\sigma^2(t)$, is defined as

$$\sigma^2(t)=Var(X-t|X>t)=\frac{2}{\bar{F}(t)}\int_t^\infty \mathrm{d}v\int_v^\infty \bar{F}(u)\mathrm{d}u-\mu^2(t),$$

where

$$\mu(t)=E(X-t|X>t)=\int_t^\infty\frac{\bar{F}(x)}{\bar{F}(t)}\mathrm{d}x$$

represents the mean residual lifetime (MRL).

Theorem 3.4. *Let X_t be the residual lifetime of X, assuming a finite $\mu(t)$ and e $\sigma^2(t)$. Then, the lower bound of $VJ^x(X;t)$ is given by*

$$VJ^x(X;t) \geq \frac{\sigma^2(t)}{4}\left\{E(-\eta_t(X_t)f_t(X_t)) - E\left(\eta_t(X_t)X_t f_t'(X_t)\right)\right\}^2,$$

where $\eta_t(x)$ satisfies

$$\sigma^2(t)\eta_t(x)f_t(x) = \int_0^x (\mu(t) - u)f_t(u)\mathrm{d}u.$$

Proof. According to [15], the next inequality holds:

$$Var(h(X)) \geq \sigma^2(E(\xi(X)h'(X)))^2,$$

where $\xi(x)$ is defined as

$$\sigma^2\xi(x)f(x) = \int_0^x (\mu(t) - u)f(u)\mathrm{d}u.$$

Let X_t denote a reference random variable satisfying $h(x) = -(xf(x))/2$. Consequently,

$$\begin{aligned} VJ^x(X;t) = Var(-\frac{1}{2}X_t f_t(X_t)) &\geq \frac{\sigma^2(t)}{4}\left\{E(\eta_t(X_t)(X_t f_t(X_t))')\right\}^2 \\ &= \frac{\sigma^2(t)}{4}\left\{E(-\eta_t(X_t)f_t(X_t)) - E\left(\eta_t(X_t)X_t f_t'(X_t)\right)\right\}^2, \end{aligned}$$

This completes the proof.

Example 3.3. Consider a random variable $X \sim \mathcal{N}(0,1)$. Let X_t denote the residual lifetime given that $X > t$, with conditional PDF $f_t(x)$. For illustration, we numerically compute and plot $\eta_t(x)$ for several fixed values of t. The resulting curves are shown in Figure 6. As observed, $\eta_t(x)$ behaves as a monotonic function with respect to x, and its shape systematically varies with t. This behavior reflects the cumulative imbalance between the conditional mean and the observed residual lifetime values up to x.

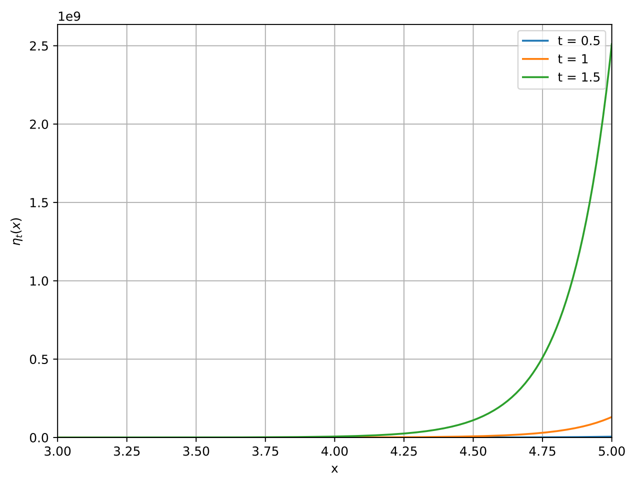

Figure 6. Variation of $\eta_t(x)$ under standard normal distribution.

Remark 3.1. *(i) If $\eta_1(t)$ is an increasing function of t, then*

$$VJ^x(X;t) \geq \frac{\sigma^2(t)}{4}\{\mathbb{E}(\eta_1(X_t)f_t(X_t))\}^2,\ t \geq 0.$$

(ii) If $f_t(x) \geq \frac{1}{x^3+1}$, then

$$VJ^x(X;t) \geq \frac{\sigma^2(t)}{4}\left\{\mathbb{E}\left(\frac{\eta_1(X_t)}{X^3+1}\right) + E\left(\eta_t(X_t)X_t f_t'(X_t)\right)\right\}^2,\ t \geq 0.$$

In the following, we investigate the behavior of WRVEx under arbitrary monotonic transformations.

Theorem 3.5. *Assume that $\phi(x)$ is a strictly monotonic, continuous, and differentiable function, and let $Y = \phi(X)$; then*

$$VJ^y(Y;t) = \begin{cases} VJ^{\frac{\varphi}{\varphi'}}(X;\varphi^{-1}(t)), & \text{if } \varphi \text{ is strictly increasing;} \\ -\frac{1}{4}E\left(\frac{\varphi^2(X_t)}{\varphi'(X_t)^2}f_t^2(X_t)\right) - J^{\frac{\varphi}{\varphi'}}(X;\varphi^{-1}(t)), & \text{if } \varphi \text{ is strictly decreasing,} \end{cases}$$

where $J^{\frac{\varphi}{\varphi'}}(X;\varphi^{-1}(t))$ and $VJ^{\frac{\varphi}{\varphi'}}(X;\varphi^{-1}(t))$ with $w(x) = \varphi(x)/\varphi'(x)$ are defined as in (1.4) *and* (3.1)*, respectively.*

Proof. Suppose $\varphi(x)$ is strictly increasing. According to (3.1), the WRVEx of $Y = \varphi(X)$ can be expressed as

$$VJ^y(Y;t) = \frac{1}{4}\left(\int_t^\infty y^2\frac{f^3(\varphi^{-1}(y))}{(\varphi'(\varphi^{-1}(y)))^3\,\bar{F}^3(\varphi(t))}\mathrm{d}y - \left(\int_t^\infty y\frac{f^2(\varphi^{-1}(y))}{(\varphi'(\varphi^{-1}(y)))^2\,\bar{F}^2(\varphi(t))}\mathrm{d}y\right)^2\right). \tag{3.2}$$

Substituting $y = \varphi(x)$ into the right-hand side of equation (3.2) and simplifying yields the result. The case where $\varphi(x)$ is strictly decreasing can be handled in a similar manner and is omitted here. □

Example 3.4. It is a well-established result that $F(X)$ follows a uniform distribution on $(0, 1)$ for any continuous random variable X. Consequently, if we define $Y = F(X)$, $VJ^w(Y;t)$ equals the WRVEx of $U(0, 1)$. Thus, we have

$$VJ^w(Y;t) = VJ^{\frac{F}{F'}}(X;F^{-1}(t)). \tag{3.3}$$

Suppose that X follows an exponential distribution with CDF $F(x) = 1 - e^{-\theta x},\ \theta > 0$. Then, $F^{-1}(t) = -\frac{\log(1-t)}{\theta}$. By (3.3), we obtain that $VJ^w(Y;t) = \frac{1}{48}$, which is the WRVEx of $U(0, 1)$.

Next, we examine the WRVEx for the PHR model. A random variable X follows the PHR model if its survival function takes the form $\bar{F}_X(x) = \bar{F}^\lambda(x)$ for $\lambda > 0$. The PDF of X is

$$g(x) = \lambda\bar{F}^{\lambda-1}(x)f(x) = \lambda\bar{F}^\lambda(x)r(x),\ \lambda > 0, \tag{3.4}$$

where λ is the proportional parameter, $\bar{F}(x)$ represents the baseline survival distribution, $f(x)$ is the baseline PDF, and $r(x) = f(x)/\bar{F}(x)$ is the baseline hazard rate function, which is well-defined on the support where $\bar{F}(x) > 0$. The PHR model is a highly flexible family of distributions that has found extensive use in reliability and survival analysis. It includes well-known distributions such as the exponential, Weibull, and Pareto distributions as special cases. For more applications of the PHR model, see [16–18].

Theorem 3.6. *Let Y have the PDF given by* (3.4)*; then the WRVEx of Y is*

$$\begin{aligned} VJ^x(Y;t) &= \frac{\lambda^4}{4\bar{F}^{3\lambda}(t)}\int_0^{\bar{F}^\lambda(t)}(\bar{F}^{-1}(y^{\frac{1}{\lambda}}))^2\Big(yr(\bar{F}^{-1}(y^{\frac{1}{\lambda}}))\Big)^4\mathrm{d}y \\ &\quad -\frac{\lambda^6}{4\bar{F}^{4\lambda}(t)}\Big(\int_0^{\bar{F}^\lambda(t)}\bar{F}^{-1}(y^{\frac{1}{\lambda}})\Big(yr(\bar{F}^{-1}(y^{\frac{1}{\lambda}}))\Big)^3\mathrm{d}y\Big)^2, \end{aligned}$$

where $y=\bar{F}^\lambda(x)$, and $\bar{F}^{-1}\left(y^{\frac{1}{\lambda}}\right)=\sup\left\{x:\bar{F}(x)\geq y^{\frac{1}{\lambda}}\right\}$ is the quantile function of $\bar{F}(x)$.

Proof. From (3.1), the WRVEx of Y is

$$VJ^x(Y;t)=\frac{1}{4}\Big(\int_t^\infty x^2\left(\frac{g(x)}{\bar{G}(t)}\right)^3\mathrm{d}x-\Big(\int_t^\infty x\left(\frac{g(x)}{\bar{G}(t)}\right)^2\mathrm{d}x\Big)^2\Big).$$

Since $y=\bar{F}^\lambda(x)$, we have

$$\begin{aligned} VJ^x(Y;t) &= \frac{1}{4\bar{F}^{3\lambda}(t)}\int_0^{\bar{F}^\lambda(t)}(\bar{F}^{-1}(y^{\frac{1}{\lambda}}))^2\left(\lambda y^{1-\frac{1}{\lambda}}f(\bar{F}^{-1}(y^{\frac{1}{\lambda}}))\right)^4\mathrm{d}y \\ &\quad -\frac{1}{4\bar{F}^{4\lambda}(t)}\Big(\int_0^{\bar{F}^\lambda(t)}\bar{F}^{-1}(y^{\frac{1}{\lambda}})\Big(\lambda y^{1-\frac{1}{\lambda}}f(\bar{F}^{-1}(y^{\frac{1}{\lambda}}))\Big)^3\mathrm{d}y\Big)^2 \\ &= \frac{\lambda^4}{4\bar{F}^{3\lambda}(t)}\int_0^{\bar{F}^\lambda(t)}(\bar{F}^{-1}(y^{\frac{1}{\lambda}}))^2\Big(yr(\bar{F}^{-1}(y^{\frac{1}{\lambda}}))\Big)^4\mathrm{d}y \\ &\quad -\frac{\lambda^6}{4\bar{F}^{4\lambda}(t)}\Big(\int_0^{\bar{F}^\lambda(t)}\bar{F}^{-1}(y^{\frac{1}{\lambda}})\Big(yr(\bar{F}^{-1}(y^{\frac{1}{\lambda}}))\Big)^3\mathrm{d}y\Big)^2. \end{aligned}$$

This completes the proof.

4. WVEx of coherent systems

This section focuses on analyzing the WVEx of coherent systems. A system is considered coherent if its structure function τ increases with respect to each component, and all components are essential. In other words, improving the performance of any individual component cannot reduce the overall lifetime of the system. Coherent systems play a crucial role in various real-world applications, such as industrial machinery, telecommunications networks, and oil pipeline infrastructures. Let T represent the lifetime of a coherent system whose components have dependent, identically distributed lifetimes denoted by X, with CDF $F(x)$ and PDF $f(x)$. Then the CDF of T is

$$F_T(x)=q(F(x)),$$

where $q:[0,1]\rightarrow[0,1]$ denotes a distortion function that only depends on the structure function and survival copula. Additionally, let h be an increasing continuous function defined on the interval $[0,1]$ such that $h(0)=0$ and $h(1)=1$. To simplify, let $u=F(x)$ and denote

$$\beta_{1,u}=\sup_{u\in[0,1]}\frac{\phi(q(u))}{\phi(u)},\ \phi(u)=\left(F^{-1}(u)\right)^2\left(f(F^{-1}(u))\right)^3,\ \text{and}\ \psi(u)=F^{-1}(u)\left(f(F^{-1}(u))\right)^2,$$

then the WVEx of T is given by

$$\begin{aligned} VJ^x(T) &= \frac{1}{4}\Big(\int_0^\infty x^2 f_T^3(x)\mathrm{d}x - \Big(\int_0^\infty x f_T^2(x)\mathrm{d}x\Big)^2\Big) \\ &= \frac{1}{4}\Big(\int_0^\infty \phi(F_T(x))\mathrm{d}x - \Big(\int_0^\infty \psi(F_T(x))\mathrm{d}x\Big)^2\Big) \\ &= \frac{1}{4}\Big(\int_0^\infty \phi(q(F(x)))\mathrm{d}x - \Big(\int_0^\infty \psi(q(F(x)))\mathrm{d}x\Big)^2\Big) \\ &= \frac{1}{4}\Big(\int_0^1 \frac{\phi(q(u))}{f(F^{-1}(u))}\mathrm{d}u - \Big(\int_0^1 \frac{\psi(q(u))}{f(F^{-1}(u))}\mathrm{d}u\Big)^2\Big), \end{aligned} \tag{4.1}$$

where $f_T(x)$ is PDF of T.

The next result provides the relationship between the WVExs of the lifetimes of a coherent system and its components. The proof is straightforward and thus is omitted for brevity.

Theorem 4.1. Suppose that $\phi(q(u)) \geq (\leq)\ \phi(u)$ and $\psi(q(u)) \leq (\geq)\ \psi(u)$; then

$$VJ^x(T) \geq (\leq) VJ^x(X).$$

Proof. From (4.1), we have

$$VJ^x(T) = \frac{1}{4}\left(\int_0^1 \frac{\phi(q(u))}{f(F^{-1}(u))}\mathrm{d}u - \left(\int_0^1 \frac{\psi(q(u))}{f(F^{-1}(u))}\mathrm{d}u\right)^2\right),$$

and similarly,

$$VJ^x(X) = \frac{1}{4}\left(\int_0^1 \frac{\phi(u)}{f(F^{-1}(u))}\mathrm{d}u - \left(\int_0^1 \frac{\psi(u)}{f(F^{-1}(u))}\mathrm{d}u\right)^2\right).$$

Suppose that $\phi(q(u)) \geq (\leq)\phi(u)$ and $\psi(q(u)) \leq (\geq)\psi(u)$ for all $u \in (0, 1)$, and noting that $f(F^{-1}(u)) > 0$, we observe

- Since $\phi(q(u)) \geq (\leq)\phi(u)$, it follows that

$$\frac{\phi(q(u))}{f(F^{-1}(u))} \geq (\leq) \frac{\phi(u)}{f(F^{-1}(u))},$$

  and thus,

$$\int_0^1 \frac{\phi(q(u))}{f(F^{-1}(u))}\mathrm{d}u \geq (\leq) \int_0^1 \frac{\phi(u)}{f(F^{-1}(u))}\mathrm{d}u.$$

- Similarly, since $\psi(q(u)) \leq (\geq)\psi(u)$, we have

$$\frac{\psi(q(u))}{f(F^{-1}(u))} \leq (\geq) \frac{\psi(u)}{f(F^{-1}(u))},$$

  and hence,

$$\left(\int_0^1 \frac{\psi(q(u))}{f(F^{-1}(u))}\mathrm{d}u\right)^2 \leq (\geq) \left(\int_0^1 \frac{\psi(u)}{f(F^{-1}(u))}\mathrm{d}u\right)^2.$$

Combining the above two inequalities yields

$$VJ^x(T) \geq (\leq) VJ^x(X),$$

which completes the proof. □

Theorem 4.1 establishes a comparison between the WVEx of the system and that of individual components. When the distortion function $q(u)$ satisfies certain conditions, the system's WVEx is bounded above or below by that of its components. This indicates that the variability in system lifetime, as captured by WVEx, can either increase or decrease depending on the dependence structure among the components.

The following Theorem 4.2 establishes an upper bound for the WVEx of coherent systems in relation to WEx.

Theorem 4.2. *If*

$$\frac{1}{x^3+3} \leq f(x) \leq 1,$$

then

$$VJ^x(T) \leq \beta_{1,u} J^{w_1}(X),$$

where $J^{w_1}(X)$ is the WEx with $w_1(x) = x^2$.

Proof. From (4.1), it can be inferred that

$$\begin{aligned}
VJ^x(T) &= \frac{1}{4}\Bigg(\int_0^1 \frac{\phi(q(u))}{f(F^{-1}(u))} \mathrm{d}u - \Bigg(\int_0^1 \frac{\psi(q(u))}{f(F^{-1}(u))} \mathrm{d}u \Bigg)^2 \Bigg) \\
&= \frac{1}{4}\Bigg(\int_0^1 \frac{\phi(q(u))}{\phi(u)} \frac{\phi(u)}{f(F^{-1}(u))} \mathrm{d}u - \Bigg(\int_0^1 \frac{\psi(q(u))}{f(F^{-1}(u))} \mathrm{d}u \Bigg)^2 \Bigg) \\
&\leq \frac{1}{4} \sup_{u\in[0,1]} \frac{\phi(q(u))}{\phi(u)} \int_0^1 \frac{\phi(u)}{f(F^{-1}(u))} du \\
&\leq \frac{1}{4}\beta_{1,u} \int_0^\infty x^2 f^2(x) \mathrm{d}x \\
&= -\frac{1}{2}\beta_{1,u} J^{w_1}(X).
\end{aligned}$$

Thus, we complete the proof.

The next corollary, directly derived from Theorem 4.1, establishes a bound for the WVEx of a coherent system.

Corollary 4.1. *If $f(x)$ satisfies the condition in Theorem 4.1, then*

$$VJ^x(T) \leq \beta_{1,u} VJ^x(X) + \beta_{1,u} (J^x(X))^2.$$

The next corollary establishes an upper bound for $VJ^x(T)$.

Corollary 4.2. *If the PDF $f(x)$ of component lifetimes satisfies $f(x) \geq L > 0$, then*

$$VJ^x(T) \leq \frac{1}{4L} \int_0^1 \phi(q(u)) \mathrm{d}u.$$

The derived bounds involving $\beta_{1,u}$ and L provide practical tools for system designers and reliability engineers. They allow for estimating the WVEx of the system without fully specifying the joint distribution of component lifetimes, provided some information on marginal distributions and the copula structure is available.

5. Non-parametric estimation of WVEx and WRVEx

We introduce non-parametric estimators for WVEx and WRVEx. To achieve this, we utilize the well-known kernel density estimator for $f(x)$, as proposed by [19]. The estimator is mathematically described as

$$\widehat{f_n}(x) = \frac{1}{nb_n} \sum_{j=1}^{n} k\left(\frac{x - X_j}{b_n}\right), \tag{5.1}$$

where $k(x)$ denotes the kernel function such that

(i) $k(x) \geq 0$ for all x;
(ii) $\int k(x)\mathrm{d}x = 1$;
(iii) $k(x)$ is symmetric about zero;
(iv) $k(x)$ satisfies the Lipschitz condition, i.e., there exists a constant M such that $|k(x)-k(y)| \leq M|x-y|$.

The following important properties of $\widehat{f_n}(x)$ and $\widehat{\bar{F}}_n(t) = \int_t^\infty \widehat{f_n}(x)\mathrm{d}x$ as given in [20] is useful to obtain our main results.

$$\mathrm{Bias}\,(\widehat{f_n}(x)) \simeq \frac{b_n c_s}{s!} f^{(s)}(x), \quad \mathrm{Var}\,(\widehat{f_n}(x)) \simeq \frac{C_k}{nb_n} f(z), \tag{5.2}$$

$$\mathrm{Bias}\,(\widehat{\bar{F}}_n(t)) \simeq \int_t^\infty f^{(s)}(x)\mathrm{d}x, \quad \mathrm{Var}\,(\widehat{\bar{F}}_n(t)) \simeq \frac{C_k}{nb_n} \bar{F}(t), \tag{5.3}$$

where $c_s = \int_{-\infty}^\infty u^s K(u)\mathrm{d}u$, $C_k = \int_{-\infty}^\infty k^2(u)\mathrm{d}u$, and $f^{(s)}(x)$ is the sth derivative of f with respect to x.

Now, we construct non-parametric estimators for WVEx and WRVEx.

Definition 5.1. *The non-parametric estimators for WVEx and WRVEx with weight $w(x) = x$ are*

$$\widehat{VJ}_n^w(X) = \frac{1}{4}\left(\int_0^\infty x^2 \widehat{f}_n^3(x)\mathrm{d}x - \left(\int_0^\infty x \widehat{f}_n^2(x)\mathrm{d}x \right)^2 \right) \tag{5.4}$$

and

$$\widehat{VJ}_n^w(X;t) = \frac{1}{4}\left(\int_t^\infty x^2 \left(\frac{\widehat{f_n}(x)}{\widehat{\bar{F}}_n(t)} \right)^3 \mathrm{d}x - \left(\int_t^\infty x \left(\frac{\widehat{f_n}(x)}{\widehat{\bar{F}}_n(t)} \right)^2 \mathrm{d}x \right)^2 \right), \tag{5.5}$$

respectively.

The non-parametric estimators given in Eqs (5.4) and (5.5) are based on a kernel density estimation framework. It is well known that, under standard regularity conditions, the choice of kernel function has a relatively minor impact on the overall performance of the estimator, provided the kernel is a valid probability density function (e.g., symmetric and integrating to one). Popular choices such as the

Gaussian, Epanechnikov, and uniform kernels generally yield similar results. Therefore, for practical purposes, we recommend using the Gaussian kernel due to its smoothness and widespread acceptance.

In contrast, the choice of bandwidth is critically important and has a significant influence on the estimator's performance. A bandwidth that is too small leads to a highly variable estimator with large variance, while an excessively large bandwidth produces an over-smoothed estimator with substantial bias. To select an appropriate bandwidth, methods such as cross-validation or Silverman's rule can be employed.

Next, we examine the consistency of the estimators for $VJ^w(X)$ and $VJ^w(X;t)$.

Theorem 5.1. The non-parametric kernel estimators $\widehat{VJ}_n^w(X)$ and $\widehat{VJ}_n^w(X;t)$ serve as consistent estimators for $VJ^w(X)$ and $VJ^w(X;t)$, respectively.

Proof. For convenience, we define

$$\widehat{h}_n(t) = \int_t^\infty x^2 \widehat{f}_n^3(x)\mathrm{d}x, \quad h(t) = \int_t^\infty x^2 f^3(x)\mathrm{d}x, \quad \widehat{m}_n(t) = \widehat{\bar{F}}_n^3(t) \text{ and } m(t) = \bar{F}^3(t),$$

thus, we have

$$\frac{1}{4}\int_t^\infty x^2\Big(\frac{\widehat{f}_n(x)}{\widehat{\bar{F}}_n(t)}\Big)^3 \mathrm{d}x = \frac{1}{4}\frac{\widehat{h}_n(t)}{\widehat{m}_n(t)}.$$

Applying the Taylor series approximation, it follows that

$$\widehat{\bar{F}}_n^3(x) = \bar{F}^3(x) + 3\bar{F}^2(x)\left(\widehat{\bar{F}}_n(x) - \bar{F}(x)\right) + 3\bar{F}(x)\left(\widehat{\bar{F}}_n(x) - \bar{F}(x)\right)^2 + o\left(\widehat{\bar{F}}_n(x) - \bar{F}(x)\right)^3$$

and

$$\widehat{f}_n^3(x) = f^3(x) + 3f^2(x)\left(\widehat{f}_n(x) - f(x)\right) + 3f(x)\left(\widehat{f}_n(x) - f(x)\right)^2 + o\left(\widehat{f}_n(x) - f(x)\right)^3.$$

As a result,

$$\widehat{h}_n(t) - h(t) = 3\int_t^\infty x^2\left(f^2(x)\left(\widehat{f}_n(x) - f(x)\right) + f(x)\left(\widehat{f}_n(x) - f(x)\right)^2\right)\mathrm{d}x$$

and

$$\widehat{m}_n(t) - m(t) = 3\left(\bar{F}^2(t)\left(\widehat{\bar{F}}_n(t) - \bar{F}(t)\right) + \bar{F}(x)\left(\widehat{\bar{F}}_n(t) - \bar{F}(t)\right)^2\right) + o\left(\widehat{\bar{F}}_n(t) - \bar{F}(t)\right)^3.$$

Thus, we have

$$\begin{aligned}
\mathrm{Bias}\,(\widehat{h}_n(t)) &\simeq 3\int_t^\infty x^2\left(f^2(x)\,\mathrm{Bias}\,(\widehat{f}_n(x)) + f(x)\,\mathrm{Bias}^2\,(\widehat{f}_n(x))\right)\mathrm{d}x,\\
\mathrm{Var}\,(\widehat{h}_n(t)) &\simeq 9\int_t^\infty \left(x^4 f^4(x)\,\mathrm{Var}\,(\widehat{f}_n(x)) + x^4 f^2(x)\,\mathrm{Var}^2\,(\widehat{f}_n(x))\right)\mathrm{d}x,\\
\mathrm{Bias}\,(\widehat{m}_n(t)) &\simeq 3\bar{F}^2(x)\,\mathrm{Bias}\,(\widehat{\bar{F}}_n(t)) + 3\bar{F}(x)\,\mathrm{Bias}^2\,(\widehat{\bar{F}}_n(t)),\\
\mathrm{Var}\,(\widehat{m}_n(t)) &\simeq 9\bar{F}^4(x)\,\mathrm{Var}\,(\widehat{\bar{F}}_n(t)) + 9\bar{F}^2(x)\,\mathrm{Var}^2\,(\widehat{\bar{F}}_n(t)).
\end{aligned}$$

By applying conditions (5.2) and (5.3) and noting that $b_n \to 0$ and $nb_n \to \infty$ as $n \to \infty$, bias and variance of $\widehat{h}_n(t)$ and $\widehat{m}_n(t)$ approach zero as $n \to \infty$. Thus, as $n \to \infty$,

$$\mathrm{MSE}(\widehat{h}_n(t)) \to 0 \text{ and } \mathrm{MSE}\,(\widehat{m}_n(t)) \to 0.$$

It follows that, $\widehat{h}_n(t) \xrightarrow{p} h(t)$ and $\widehat{m}_n(t) \xrightarrow{p} m(t)$, as $n \to \infty$. Applying Slutsky's theorem gives

$$\frac{1}{4}\int_t^\infty x^2\Big(\frac{\widehat{f}_n(x)}{\widehat{\bar{F}}_n(t)}\Big)^3 \mathrm{d}x = \frac{1}{4}\frac{\widehat{h}_n(t)}{\widehat{m}_n(t)} \xrightarrow{p} \frac{1}{4}\frac{h(t)}{m(t)} = \frac{1}{4}\int_t^\infty x^2\left(\frac{f(x)}{\bar{F}(t)}\right)^3 \mathrm{d}x.$$

According to Theorem 5 of [4], $\widehat{J}_n^w(X;t)$ converges in probability to $J^w(Z;t)$; thus

$$\Big(\int_t^\infty x\Big(\frac{\widehat{f}_n(x)}{\widehat{\bar{F}}_n(t)}\Big)^2 \mathrm{d}x\Big)^2 \xrightarrow{p} \Big(\int_t^\infty x\left(\frac{f(x)}{\bar{F}(t)}\right)^2 \mathrm{d}x\Big)^2.$$

Hence, $\widehat{VJ}_n^w(X;t)$ serves as a consistent estimator of $VJ^w(Z;t)$, and the consistency of $\widehat{VJ}_n^w(X)$ can be shown similarly and is omitted here.

The next theorem addresses the asymptotic normality of $\widehat{VJ}_n^w(X)$and $\widehat{VJ}_n^w(X;t)$.

Theorem 5.2. *Let $\widehat{VJ}_n^w(X)$ and $\widehat{VJ}_n^w(X;t)$ denote the non-parametric kernel estimators for $VJ^w(X)$ and $VJ^w(X;t)$, respectively. Assume that the kernel function $k(\cdot)$ is a symmetric probability density function with compact support, bounded variation, and continuous first derivative. As $n \to \infty$, for a fixed t, both*

$$(nb_n)^{\frac{1}{2}}\Big(\frac{\widehat{VJ}_n^w(X) - VJ^w(X)}{\sigma_1}\Big) \text{ and } (nb_n)^{\frac{1}{2}}\Big(\frac{\widehat{VJ}_n^\omega(X;t) - VJ^w(X;t)}{\sigma_2}\Big)$$

follow a standard normal distribution, where

$$\sigma_1^2 = C_k\int_0^\infty f(x)\Big(\frac{3}{4}x^2 f^2(x) - xf(x)\int_0^\infty tf^2(t)\mathrm{d}t\Big)^2 \mathrm{d}x,$$

$$\sigma_2^2 = \frac{C_k}{\bar{F}^6(t)}\Big(h(t)h_1(t) + 2\bar{F}^3(t)h_1^3(t) + 9\int_t^\infty x^4 f^5(x)\mathrm{d}x + \frac{9h(t)}{\bar{F}(t)}\Big),$$

and $h_1(t) = \int_t^\infty xf^2(x)\mathrm{d}x$.

Proof. We start by noting that

$$\begin{aligned}
\widehat{VJ}_n^w(X) &= \frac{1}{4}\Big(\int_0^\infty x^2\widehat{f}_n^3(x)\mathrm{d}x - \Big(\int_0^\infty x\widehat{f}_n^2(x)\mathrm{d}x\Big)^2\Big) \\
&= \frac{1}{4}\int_0^\infty x^2\widehat{f}_n^3(x)\mathrm{d}x - \frac{1}{4}\Big(\int_0^\infty x\widehat{f}_n^2(x)\mathrm{d}x - \int_0^\infty xf^2(x)\mathrm{d}x\Big)^2 + \frac{1}{4}\Big(\int_0^\infty xf^2(x)\mathrm{d}x\Big)^2 \\
&\quad -\frac{1}{2}\int_0^\infty xf^2(x)\mathrm{d}x\Big(\int_0^\infty x\widehat{f}_n^2(x)\mathrm{d}x - \int_0^\infty xf^2(x)\mathrm{d}x\Big).
\end{aligned}$$

Using Taylor series expansion, it follows that

$$\int_0^\infty \widehat{f}_n^\alpha(x)\mathrm{d}x - \int_0^\infty f^\alpha(x)\mathrm{d}x \simeq \alpha\int_0^\infty f^{\alpha-1}(x)(\widehat{f}_n(x) - f(x))\mathrm{d}x, \quad \alpha = 1,2,3.$$

Thus, it follows that

$$\begin{aligned}\widehat{VJ}_n^w(X) &\simeq \frac{1}{4}\int_0^\infty x^2 f^3(x)\mathrm{d}x + \frac{3}{4}\int_0^\infty x^2 f^2(x)(\widehat{f_n}(x) - f(x))\mathrm{d}x - \left(\int_0^\infty xf(x)(\widehat{f_n}(x) - f(x))\mathrm{d}x\right)^2 \\ &\quad + \frac{1}{4}\left(\int_0^\infty xf^2(x)\mathrm{d}x\right)^2 - \int_0^\infty xf^2(x)\mathrm{d}x \int_0^\infty xf(x)(\widehat{f_n}(x) - f(x))\mathrm{d}x,\end{aligned}$$

and hence,

$$\begin{aligned}&\sqrt{nb_n}(\widehat{VJ}_n^w(X) - \widehat{VJ}^w(X)) \\ \simeq\ &\sqrt{nb_n}\Big(\frac{3}{4}\int_0^\infty x^2 f^2(x)(\widehat{f_n}(x) - f(x))\mathrm{d}x - \left(\int_0^\infty x\widehat{f_n^2}(x)\mathrm{d}x - \int_0^\infty xf^2(x)\mathrm{d}x\right)^2 \\ &- \int_0^\infty xf^2(x)\mathrm{d}x \int_0^\infty xf(x)(\widehat{f_n}(x) - f(x))\mathrm{d}x\Big) \\ =\ &\sqrt{nb_n}\int_0^\infty (\widehat{f_n}(x) - f(x))\Big(\frac{3}{4}x^2 f^2(x) - xf(x)\int_0^\infty tf^2(t)\mathrm{d}t\Big)\mathrm{d}x + o_p(1),\end{aligned}$$

where the final equality is derived by Theorem 3.4 in [21]. By the asymptotic normality of $\widehat{f_n}(x)$ established in [22], we can directly conclude that

$$\sigma_1^2 = C_k \int_0^\infty f(x)\Big(\frac{3}{4}x^2 f^2(x) - xf(x)\int_0^\infty tf^2(t)\mathrm{d}t\Big)^2 \mathrm{d}x.$$

Following a similar approach, we can obtain the asymptotic normality of $\widehat{VJ}_n^w(X;t)$, which is omitted for brevity.

In the following, we employ Monte Carlo simulations to analyze the behavior of the WVEx and WRVEx estimators, as defined in Eqs (5.4) and (5.5), respectively. The simulations are conducted using an exponential distribution with $\lambda = 1$. For the estimation process, we utilize the Gaussian kernel $k(z) = \frac{1}{\sqrt{2\pi}}e^{-z^2/2}$. The estimators are assessed across various values of t, bandwidth b_n, and sample sizes $n = 40, 50, 100$. For each combination of t and b_n, the simulation is repeated 5000 times to ensure robust results. The accuracy of the estimators is measured using bias, standard deviations (SD), and mean squared error (MSE). The results of the WVEx and WRVEx estimators are presented in Tables 2 and 3, respectively.

Tables 2 and 3 show that for both WVEx and WVREx, increasing the sample size results in improved performance, with smaller bias, SD, and MSE, indicating better accuracy and reduced estimation errors. Larger bandwidth values can lead to increased standard deviation and mean squared error, suggesting that choosing an appropriate bandwidth is crucial. Larger bandwidths may increase the variability of the estimates, making it essential to balance between bandwidth and estimation stability.

Table 2. Bias, SD, and MSE of the WVEx for fixed bandwidth.

n	$b_n = 0.5$			$b_n = 0.7$			$b_n = 0.9$		
	Bias	SD	MSE	Bias	SD	MSE	Bias	SD	MSE
40	0.002750	0.001241	0.000009	0.002869	0.001024	0.000009	0.002818	0.000852	0.000009
50	0.002658	0.001089	0.000008	0.002818	0.000903	0.000009	0.002785	0.000752	0.000008
100	0.002496	0.000768	0.000007	0.002733	0.000638	0.000008	0.002733	0.000528	0.000008

Table 3. Bias, SD, and MSE of the WVREx for fixed bandwidth.

n	t	$b_n = 0.5$			$b_n = 0.7$			$b_n = 0.9$		
		Bias	SD	MSE	Bias	SD	MSE	Bias	SD	MSE
40	0.5	-0.023646	0.015354	0.000795	-0.001988	0.002441	0.000010	0.002616	0.001188	0.000008
	0.7	-0.003232	0.009215	0.000095	0.002184	0.003026	0.000014	0.002763	0.001756	0.000011
	0.9	0.004743	0.005789	0.000056	0.002965	0.003629	0.000022	0.000814	0.002305	0.000006
50	0.5	-0.022522	0.012834	0.000672	-0.001859	0.002156	0.000008	0.002631	0.001075	0.000008
	0.7	-0.002587	0.007706	0.000066	0.002275	0.002703	0.000012	0.002772	0.001576	0.000010
	0.9	0.004816	0.005071	0.000049	0.002968	0.003235	0.000019	0.000800	0.002060	0.000005
100	0.5	-0.020418	0.007658	0.000476	-0.001610	0.001449	0.000005	0.002672	0.000768	0.000008
	0.7	-0.001448	0.004499	0.000022	0.002444	0.001884	0.000010	0.002799	0.001129	0.000009
	0.9	0.004906	0.003603	0.000037	0.002983	0.002332	0.000014	0.000791	0.001482	0.000003

Subsequently, we implemented Silverman's rule to automatically determine the bandwidth based on each generated sample. This approach is particularly useful in real-world applications where data variability is high and bandwidth selection is crucial for model accuracy. The results presented in Tables 4 and 5 demonstrate that, as the sample size increases, the bias, SD, and MSE of both the WVEx and WRVEx estimators generally decrease, indicating improved estimation accuracy.

Table 4. Bias, SD, and MSE of the WVEx for bandwidth selected by Silverman's rule.

n	Bias	SD	MSE
40	0.002604	0.001586	0.000009
50	0.002384	0.001357	0.000008
100	0.001889	0.000901	0.000004

Table 5. Bias, SD, and MSE of the WVREx for bandwidth selected by Silverman's rule.

n	t	Bias	SD	MSE
40	0.5	-0.117707	1.752359	3.084615
	0.7	-0.019583	0.624645	0.390565
	0.9	0.004404	0.011882	0.000161
50	0.5	-0.067621	0.380519	0.149367
	0.7	-0.012594	0.313122	0.098204
	0.9	0.004786	0.007094	0.000073
100	0.5	-0.056758	0.080122	0.009641
	0.7	-0.005867	0.012762	0.000197
	0.9	0.005273	0.004499	0.000048

6. A real data

A real-world data set concerning COVID-19 infections is analyzed in this section, where data for 42 countries were gathered from various official sources as of March 26, 2020. Below is the detailed information of the data set: 1.56, 8.51, 2.17, 0.37, 1.09, 9.84, 4.95, 3.18, 11.37, 2.81, 6.22, 1.87, 9.05, 2.44, 1.38, 4.17, 3.74, 1.37, 2.33, 7.80, 2.10, 0.47, 2.54, 4.92, 0.09, 0.18, 1.72, 1.02, 0.62, 2.34, 0.50, 2.37, 3.65, 0.59, 5.76, 2.14, 0.88, 0.95, 4.17, 2.25. Kasilingam [23] applied an exponential model to analyze the transmission of COVID-19. Recently, Kayid [10] studied the data set; they compared the theoretical values of residual extropy with their corresponding estimates and observed that the data set closely fits an exponential distribution with an estimated parameter $\hat{\lambda} = 0.32$. Here, we investigate the proximity of the WVEx and WRVEx estimators to their corresponding theoretical values, and no normalization or transformation was applied to the dataset before estimation. A range of combinations for t and b_n are provided in Tables 6 and 7, which reveal that the WVEx and WRVEx estimators approach the theoretical values as b_n increases.

Table 6. Theoretical values and corresponding estimates of WVEx.

	$b_n = 0.1$	$b_n = 0.3$	$b_n = 0.5$	$b_n = 0.7$	$b_n = 0.9$
$\widehat{VJ}_n^w(X)$	0.027771	0.007991	0.005479	0.005012	0.004975
$VJ^w(X)$	0.002894	0.002894	0.002894	0.002894	0.002894

Table 7. Theoretical values and corresponding estimates of WRVEx.

	t	$b_n = 0.3$	$b_n = 0.5$	$b_n = 0.7$	$b_n = 0.9$
$\widehat{VJ}_n^w(X;t)$	0.3	0.004085	0.002529	0.002892	0.003448
$VJ^w(X;t)$		0.002419	0.002419	0.002419	0.002419
$\widehat{VJ}_n^w(X;t)$	0.5	0.003082	0.002016	0.002667	0.003376
$VJ^w(X;t)$		0.002316	0.002316	0.002316	0.002316
$\widehat{VJ}_n^w(X;t)$	0.7	0.005146	0.002614	0.002976	0.003656
$VJ^w(X;t)$		0.002383	0.002383	0.002383	0.002383
$\widehat{VJ}_n^w(X;t)$	0.9	0.008546	0.004291	0.003923	0.004385
$VJ^w(X;t)$		0.002622	0.002622	0.002622	0.002622

Table 7 shows that both t and b_n affect the estimator's accuracy. Moderate values of t (e.g., 0.5 or 0.7) yield estimates closer to the theoretical WRVEx. For bandwidth, larger b_n (e.g., 0.7 or 0.9) reduces variance and improves stability. In applications, we recommend moderate t and data-driven bandwidth selection for balanced performance.

7. Conclusions

In this study, we have introduced the concept of the WRVEx as a valuable addition to the study of variability in uncertainty measures. We have also explored the theoretical properties of the WVEx and

WRVEx, including their behavior under monotonic transformations and the derivation of key bounds. Furthermore, we demonstrated the application of WVEx in the analysis of coherent systems and the PHR model. The kernel-based non-parametric estimators for both WVEx and WRVEx were proposed, with their effectiveness validated through simulation experiments and analysis of a real-world data set.

Author contributions

Li Zhang: Methodology, Writing–review and editing; Bin Lu: Methodology, Writing original draft. All authors have read and agreed to the published version of the manuscript.

Use of Generative-AI tools declaration

The authors declare they have not used Artificial Intelligence (AI) tools in the creation of this article.

Acknowledgments

This work was supported by the Natural Science Foundation of Gansu Province of China (No. 22JR11RA144).

Conflict of interest

The authors declare that they have no conflicts of interest.

References

1. C. E. Shannon, A mathematical theory of communication, *Bell Syst. Tech. J.*, **27** (1948), 379–423. https://doi.org/10.1002/j.1538-7305.1948.tb01338.x
2. F. Lad, G. Sanfilippo, G. Agro, Extropy: complementary dual of entropy, *Statist. Sci.*, **30** (2015), 40–58. https://doi.org/10.1214/14-STS430
3. G. X. Qiu, K. Jia, The residual extropy of order statistics, *Statist. Probab. Lett.*, **133** (2018), 15–22. https://doi.org/10.1016/j.spl.2017.09.014
4. E. I. A. Sathar, R. D. Nair, On dynamic weighted extropy, *J. Comput. Appl. Math.*, **393** (2021), 113507. https://doi.org/10.1016/j.cam.2021.113507
5. G. X. Qiu, The extropy of order statistics and record values, *Statist. Probab. Lett.*, **120** (2017), 52–60. https://doi.org/10.1016/j.spl.2016.09.016
6. A. S. Krishnan, S. M. Sunoj, N. U. Nair, Some reliability properties of extropy for residual and past lifetime random variables, *J. Korean Statist. Soc.*, **49** (2020), 457–474. https://doi.org/10.1007/s42952-019-00023-x
7. R. D. Nair, E. I. A. Sathar, Some useful results related to various measures of extropy and their interrelationship, *Statist. Probab. Lett.*, **193** (2023), 109729. https://doi.org/10.1016/j.spl.2022.109729
8. G. X. Qiu, K. Jia, Extropy estimators with applications in testing uniformity, *J. Nonparametr. Stat.*, **30** (2018), 182–196. https://doi.org/10.1080/10485252.2017.1404063

9. S. Chakraborty, B. Pradhan, On cumulative residual extropy of coherent and mixed systems, *Ann. Oper. Res.*, **340** (2024), 59–81. https://doi.org/10.1007/s10479-023-05727-2
10. M. Kayid, Further results involving residual and past extropy with their applications, *Statist. Probab. Lett.*, **214** (2024), 110201. https://doi.org/10.1016/j.spl.2024.110201
11. N. M. Vaselabadi, S. Tahmasebi, M. R. Kazemi, F. Buono, Results on varextropy measure of random variables, *Entropy*, **23** (2021), 1–14. https://doi.org/10.3390/e23030356
12. S. K. Chaudhary, N. Gupta, Extropy and varextropy estimators with applications, 2024, arXiv: 2401.13065.
13. S. Saha, S. Kayal, Weighted (residual) varentropy and its applications, *J. Comput. Appl. Math.*, **442** (2024), 115710. https://doi.org/10.1016/j.cam.2023.115710
14. M. Asadi, N. Ebrahimi, Residual entropy and its characterizations in terms of hazard function and mean residual life function, *Statist. Probab. Lett.*, **49** (2000), 263–269. https://doi.org/10.1016/S0167-7152(00)00056-0
15. T. Cacoullos, V. Papathanasiou, Characterizations of distributions by variance bounds, *Statist. Probab. Lett.*, **7** (1989), 351–356. https://doi.org/10.1016/0167-7152(89)90050-3
16. D. R. Cox, Regression models and life-tables, *J. R. Stat. Soc. Ser. B Stat. Methodol.*, **34** (1972), 187–202. https://doi.org/10.1111/j.2517-6161.1972.tb00899.x
17. R. C. Gupta, R. D. Gupta, Proportional reversed hazard rate model and its applications, *J. Statist. Plann. Inference*, **137** (2007), 3525–3536. https://doi.org/10.1016/j.jspi.2007.03.029
18. F. Belzunce, C. Martínez-Riquelme, Bounds for the hazard rate and the reversed hazard rate of the convolution of dependent random lifetimes, *J. Appl. Probab.*, **56** (2019), 1033–1043. https://doi.org/10.1017/jpr.2019.59
19. E. Parzen, On estimation of a probability density function and mode, *Ann. Math. Stat.*, **33** (1962), 1065–1076.
20. E. Masry, Recursive probability density estimation for weakly dependent stationary processes, *IEEE Trans. Inform. Theory*, **32** (1986), 254–267. https://doi.org/10.1109/TIT.1986.1057163
21. R. Rajesh, G. Rajesh, S. M. Sunoj, Kernel estimation of extropy function under length-biased sampling, *Statist. Probab. Lett.*, **181** (2022), 109290. https://doi.org/10.1016/j.spl.2021.109290
22. G. G. Roussas, Asymptotic normality of the kernel estimate under dependence conditions: application to hazard rate, *J. Statist. Plann. Inference*, **25** (1990), 81–104. https://doi.org/10.1016/0378-3758(90)90008-I
23. D. Kasilingam, S. P. S. Prabhakaran, D. K. Rajendran, V. Rajagopal, T. S. Kumar, A. Soundararaj, Exploring the growth of COVID-19 cases using exponential modelling across 42 countries and predicting signs of early containment using machine learning, *Transbound. Emerg. Dis.*, **68** (2021), 1001–1018. https://doi.org/10.1111/tbed.13764

AIMS Press